Microchim Acta (2013) 180:829–835
DOI 10.1007/s00604-013-1006-7

ORIGINAL PAPER

Fluorescent assay for oxytetracycline based on a long-chain aptamer assembled onto reduced graphene oxide

Huimin Zhao · Sheng Gao · Meng Liu · Yangyang Chang · Xinfei Fan · Xie Quan

Received: 7 February 2013 / Accepted: 15 April 2013 / Published online: 28 April 2013

Abstract We report on a fluorescent assay for oxytetracycline (OTC) using a fluorescein-labeled long-chain aptamer assembled onto reduced graphene oxide (rGO). The π-π stacking interaction between aptamer and rGO causes the fluorescence of the label to be almost completely quenched via energy transfer so that the system has very low background fluorescence. The addition of OTC leads to the formation of G-quadruplex OTC complexes and prevents the adsorption of labeled aptamer on the surface of rGO. As a result, fluorescence is restored, and this effect allows for a quantitative assay of OTC over the 0.1–2 μM concentration range and with a detection limit of 10 nM. This method is simple, rapid, selective and sensitive. It may be applied to other small molecule analytes by applying appropriate aptamers.

Keywords Long-chain aptamer · Oxytetracycline · Fluorescent assay · Graphene

Introduction

Oxytetracycline (OTC) is one of the most frequently used tetracyclines (TCs) as antibiotic growth promoters supplied with livestock feed [1]. The extensive use of TCs including OTC in veterinary medicine has led them to be accumulated in food products or be released into the soil and natural waters via animal metabolism, causing serious threats to human and environmental health [2].

Researchers have been undertaking constant efforts to detect tetracycline antibiotics in food products, pharmaceutical preparations, and natural waters. The conventional techniques that have been used so far are high performance liquid chromatography (HPLC) [3], enzyme-linked immunosorbent assays (ELISA) [4], surface-enhanced Raman scattering (SERS) [5] and capillary electrophoresis [6], which suffer from some limitations, such as long procedures and analysis time, extensive equipment, low specificity and the need of authentic samples as reference standards. Several other novel analysis methods for detecting TCs, such as amperometric detection methods [7] and antibody-based colorimetric methods [8], were found neither specific nor sensitive, resulting from the high structural similarity of derivatives. To overcome the limitations of these available techniques, considerable research efforts have been made to propel the development of rapid, accurate, and economic alternative recognition elements.

Aptamers, the artificial single-stranded DNA (ssDNA) or RNA oligonucleotides, possess the ability to form defined three-dimensional structure for specific target binding [9]. Owing to the high specific affinity to their target molecules (small molecules, proteins, and even entire cells) [10], aptamers, as promising alternative recognition elements to antibodies, have received tremendous attention in biosensing applications in recent years. Compared to antibodies, aptamers have a number of unique features, such as chemical synthesis and selection in-vitro through the systematic evolution of ligands by exponential enrichment (SELEX) process, easy modification, high stability, and anti-degradation [11]. Recently, a single-stranded DNA aptamer (76-mer) has been identified that can bind to OTC with high affinity and

Electronic supplementary material The online version of this article (doi:10.1007/s00604-013-1006-7) contains supplementary material, which is available to authorized users.

H. Zhao (✉) · S. Gao · M. Liu · Y. Chang · X. Fan · X. Quan
Key Laboratory of Industrial Ecology and Environmental Engineering (Ministry of Education, China), School of Environmental Science and Technology, Dalian University of Technology, Dalian 116024, China
e-mail: zhaohuim@dlut.edu.cn

specificity among other TC derivatives [12]. Based on this aptamer, several OTC aptasensors have been successfully constructed in connection to electrochemical [13, 14], colorimetric [15, 16], light scattering [17] and microcantilever [18] methods. For instance, Kim et al. [13] developed an electrochemical aptasensor with desirable sensitivity on a gold interdigitated array electrode for the detection of OTC. However, this method was laborious and not suitable for on-site detection, mainly ascribed to tedious immobilization steps of the aptamers on an electrode and numerous wash steps. As an alternative, Kim et al. [15, 16] designed a simple colorimetric aptasensor using gold nanoparticles as signal reporters, and the detection limit was 25 nM. Even though this colorimetric sensing system should be an attractive transducer in terms of its simplicity and high sensitivity, the method still had two of the important limiting cases due to the inherent characteristics of gold nanoparticles, which were (i) an unavoidable high background signal and (ii) metallic nanoparticles' instability in biological complex or environmental samples. In this respect, there is still an urgent need to search for new simple and sensitive aptamer-based detection methods for OTC assay.

Graphene and its derivatives, two-dimensional carbon nanosheets, have attracted wide research interest because of their unique mechanical, electrical, thermal, and optical properties [19, 20]. Owing to their peculiar electronic properties, the water-soluble graphene oxide (GO) and the surface modified graphene have acted as the highly efficient fluorescence quencher based on either electron transfer mechanism or energy transfer mechanism [21, 22]. In addition, the large two-dimensional surface of graphene can bind single-stranded DNA via hydrophobic and π-π stacking interactions between the ring structures in the nucleobases and the hexagonal cells of graphene, but it hardly interacts with rigid double-stranded DNA or aptamer-target complexes. The differential binding of ssDNA and dsDNA/structured DNA toward graphene has been used in various fluorescence assays [23, 24]. Combined the above features with their excellent capabilities for conjugation of target molecules, good biocompatibility, and low cytotoxicity [25], graphene and its derivatives have been widely used in the fluorescence sensing platforms for determination of DNA [23], proteins [26, 27], and other small molecules [28]. It is worth noting that in the previous reported graphene-based fluorescent aptasensors, the lengths of the aptamers were short (≤40-mer) and the quenchers were GO or sodium dodecylbenzene sulfonate (SDBS) dispersed graphene [23, 26–28]. To the best of our knowledge, the long-chain aptamers have been rarely applied to graphene-based fluorescent aptasensors. The reason may be that the long-chain aptamers possess unique secondary structures, which decrease the exposure of nucleobases, and thus the structured long-chain aptamers are adsorbed more slowly and bind less compactly to the surface of graphene [29, 30]. However, some targets need long-chain aptamers as recognition units [31, 32]. Therefore it is meaningful to overcome the above limitations and utilize long-chain aptamers as probes in the graphene-based fluorescence sensing platforms.

Herein, we present a simple and sensitive fluorescent assay for OTC based on regulation of the interaction between fluorescein-labeled long-chain aptamer (76-mer) and reduced graphene oxide (rGO). rGO shows good water-dispersibility and excellent quenching ability due to the exist of more crystalline graphene regions on the sheet compared with GO, which is contributed to the strong adsorption of long-chain aptamer on rGO surface. Our strategy utilizes the efficient quenching ability of rGO and the different interaction intensity of aptamer, aptamer/OTC complex with rGO which directly induces the fluorescence intensity change. This homogeneous fluorescent assay possesses excellent sensitivity and a high signal-to-noise ratio, thus laying a basis for its application in molecule recognition with long-chain aptamers.

Experimental

Reagents and chemicals

Oxytetracycline (OTC), tetracycline (TET), doxycycline (DOX), and chlortetracycline (CTC) were purchased from Aladdin Reagent Co., Ltd. (Shanghai, China, http://www.aladdin-reagent.com). Other reagents were analytical grade and purchased from Sinopharm Chemical Reagent Co., Ltd. (Shanghai, China, http://www.sinoreagent.com.cn). The fluorescein amidite (FAM) labeled OTC aptamer (OTA) with a sequence 5′-FAM-CGTACGGAATTCGCTAG-CCGAGTTGAGCCGGGCGCGGTACGGGTACTGGTAT-GTGTGGGGATCCGAGCTCCACGTG-3′, was synthesized by TaKaRa Biotechnology Co., Ltd. (Dalian, China, http://www.takara.com.cn) and purified by HPLC. Phosphate buffer solution (20 mM, pH=7.4) was prepared by mixing the stock solution of Na_2HPO_4 and NaH_2PO_4. Ultrapure water purified by a Millipore water system (resistivity > 18.0 MΩ cm^{-1}, Laikie Instrument Co., Ltd., Shanghai, China, http://www.okpure.com) was used throughout the experiments.

Characterization

Atomic force microscopy (AFM) measurements were carried out on Agilent PicoPlus II. The AFM sample was prepared by casting 5 μL of rGO dispersion on a freshly-cleaved mica surface. Transmission electron microscopy (TEM) images of rGO were measured by FEI Tecnai G2 Spirit. Fluorescence measurements were performed on a Hitachi F-4500 spectrofluorimeter. All experiments were carried out at room temperature. The fluorescence intensity

was monitored by exciting the sample at 494 nm and measuring the emission at 520 nm. The slits for excitation and emission were set at 5 nm and 10 nm respectively. The results were reported as mean values of triplicates.

Preparation of rGO

The GO sheets were prepared from graphite powder according to the modified Hummers method [33]. In detail, 1 g graphite powder was added into 23 mL concentrated H_2SO_4 with vigorous stirring at 0 °C, and then 3 g $KMnO_4$ was slowly added under the same condition. After that, the mixing substance was sonicated for 6 h to obtain a dark green solution. Successively, 46 mL H_2O was transferred into the reaction system gradually. For 15 min, then this reaction was terminated by 140 mL H_2O and 10 mL H_2O_2 (30 %). Then the yellow resultant was separated by centrifugation, and the sediment was washed by HCl (5 %) and ultrapure water in turn.

The rGO sheets were synthesized through an environment-friendly hydrothermal route [34]. Briefly, 50 mL GO aqueous solution (0.05 mg·mL^{-1}) was transferred into a Teflon-lined autoclave and heated at 180 °C for 6 h. After autoclave cooling to the room temperature, the black homogeneous rGO solution was obtained. The obtained rGO sheets could be readily dispersed in water because of the residual negatively charged oxygen functional groups at the edges.

Detection of OTC

For quantitative assay of OTC, the working solution of 1 μM FAM-labeled OTA was prepared using 20 mM phosphate buffer. Twenty μL of 1 μM FAM-labeled OTA was incubated at room temperature for 30 min after adding 50 μL appropriate concentrations of OTC in phosphate buffer (100 mM NaCl, 3 mM $MgCl_2$, 10 mM KCl, pH=7.4). Then 130 μL of 0.05 mg·mL^{-1} rGO was added to the above solution. The mixed solution was diluted with ultrapure water to 400 μL and shaken mildly for 30 min at room temperature. Finally, the fluorescence intensity was measured at 518 nm with excitation at 494 nm. Other structurally similar antibiotics such as tetracycline (TET), chlorotetracycline (CTC) and doxycycline (DOX) were also examined under the same procedure for the specificity tests.

Results and discussions

The analytical mechanism of the method

Scheme 1 illustrates the sensing strategy for the detection of OTC. In the absence of target molecules, FAM-modified long-chain aptamer is adsorbed onto the surface of rGO via hydrophobic and π-π stacking interactions between the ring structures in the nucleobases and the hexagonal cells of rGO. The interactions induce them into fluorescence resonance energy transfer (FRET) proximity, hence leading to the fluorescence quenching of dyes by rGO. Upon the addition of OTC, the high affinity between OTC and its specific long-chain aptamer leads to the formation of well-folded OTC-aptamer complex and then decreases the exposure of nucleobases, which makes the dyes away from the rGO surface, thus hindering the FRET process and producing a restoration of fluorescence.

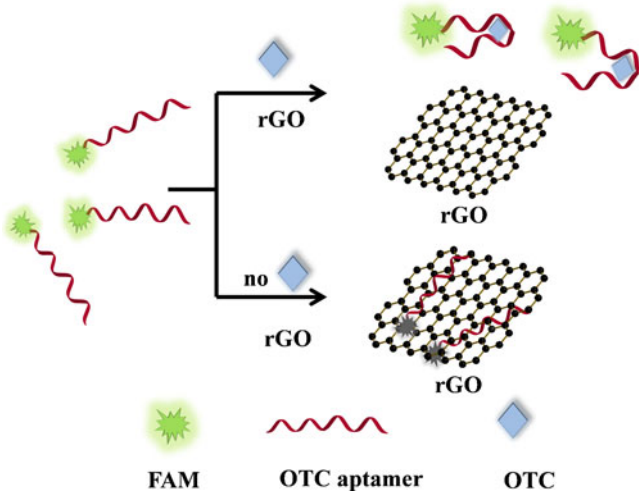

Scheme 1 Schematic illustration of this fluorescent assay for OTC based on rGO and OTC binding aptamer

Characterization of rGO

AFM was employed to characterize the morphology and thickness of a graphene sheet. A typical AFM image showed a high-quality single-layer graphene sheet with about 1 nm thickness (Fig. S1a, Electronic Supplementary Material, ESM). TEM was performed to confirm the formation of the rGO sheets. As shown in Fig. S1b (ESM), the resultant rGO was observed with occasional folds, crinkles, and rolled edges, which was typical for sheets of rGO and similar to the previous report [34], confirming the formation of rGO.

Optimization of assay conditions

Effect of salt and optimization of assay time

Since DNA was a polyanion, aptamer should be repelled by the negatively charged GO through electrostatic repulsion. Electrolytes were needed to screen the long-range electrostatic repulsion and bring aptamer close to the rGO surface for binding [28]. The kinetic behaviors of FAM-labeled aptamer and rGO were studied by monitoring the

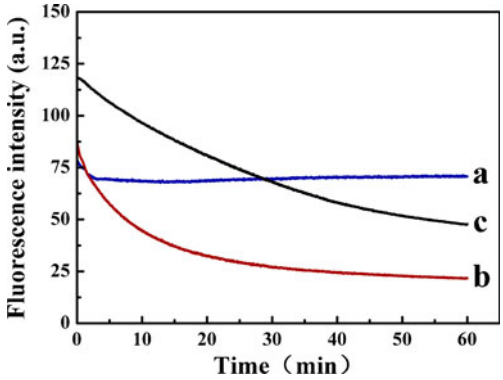

Fig. 1 FAM-labeled aptamer quenching kinetic behaviors. In (**a**), rGO concentration = 40 μg•mL^{-1} without the addition of salt. In (**b**), rGO concentration = 16 μg•mL^{-1} with 12.5 mM NaCl, 0.4 mM MgCl2. In (**c**), GO concentration = 40 μg•mL^{-1} with 12.5 mM NaCl, 0.4 mM MgCl2. The original fluorescence intensity of FAM-labeled aptamer (50 nM) without rGO was 330 a.u.. Excitation: 494 nm, emission: 518 nm

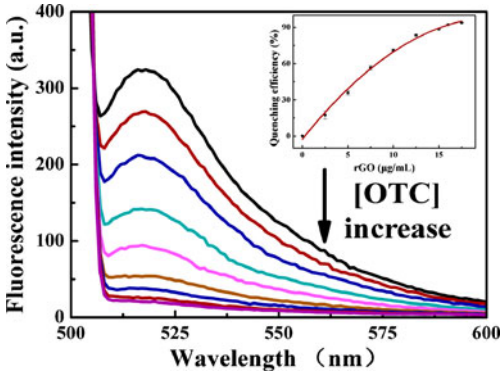

Fig. 3 Fluorescence spectra of FAM-labeled aptamer in the presence of different concentrations of rGO, with concentrations of 0, 2.5, 5, 7.5, 10, 12.5, 15, 16, 17.5 μg•mL^{-1} from top to bottom. Inset: fluorescence quenching efficiency versus concentration of rGO. Excitation: 494 nm, emission: 518 nm

fluorescence intensity as a function of time. As showed in Fig. 1 (curve a), in the absence of salt, FAM-labeled aptamer could not be completely quenched even upon the addition of high concentrations of rGO (40 μg·mL^{-1}), the quenching efficiency was ~75 %, confirming that the adsorption was limited by the repulsive interaction. A significant quenching effect (~90 %) was observed under a lower concentration of rGO (16 μg·mL^{-1}) in the presence of salt (Fig. 1 (curve b)), suggesting that the electrostatic repulsion could be shielded by the effect of salt. Moreover, the process of adsorption reached equilibrium in less than 30 min, indicating fast adsorption kinetics. In addition, under the same concentration of salt, rGO captured long-chain aptamer more efficiently and rapidly than the universal quencher GO (40 μg·mL^{-1}) (Fig. 1 (curve c)). This might result from the structure of rGO where existed more crystalline graphene regions that could bind to aptamer and less negatively charged regions containing the anionic functionalization that

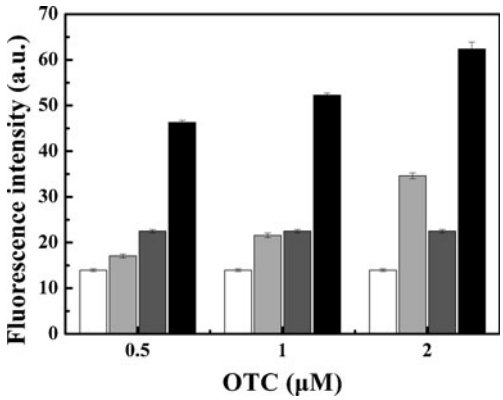

Fig. 2 The effect of K^+ on the efficiency of the fluorescence recovery. The *white bars* and the *light grey bars* represented the fluorescence intensity of FAM-labeled aptamer/rGO system before and after incubation with different concentrations of OTC in the phosphate buffer without K^+, respectively. The *dark grey bars* and the *black bars* represented the fluorescence intensity of FAM-labeled aptamer/rGO complex before and after incubation with different concentrations of OTC in the phosphate buffer with 10 mM K^+, respectively. Excitation: 494 nm, emission: 518 nm

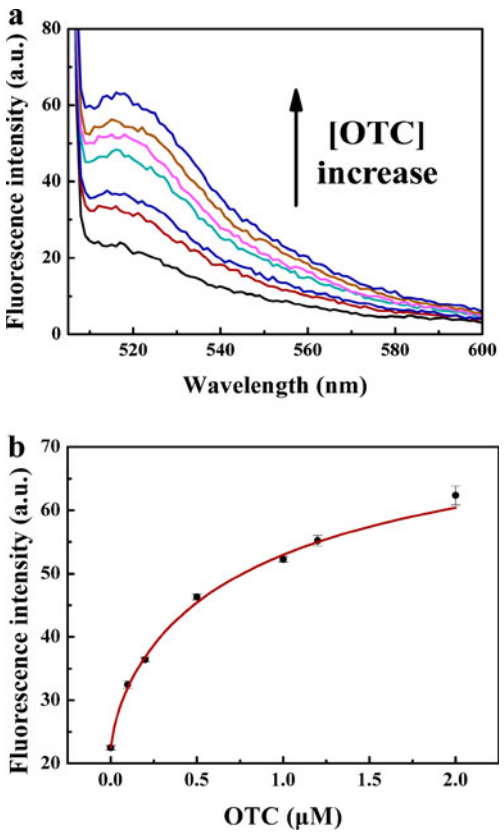

Fig. 4 **a** Fluorescence emission spectra upon increasing the concentration of OTC, with concentrations of 0, 0.1, 0.2, 0.5, 1, 1.2, 2 μM from bottom to top. **b** Plot of the fluorescence intensity against the concentration of OTC. Excitation: 494 nm, emission: 518 nm

Table 1 Comparison of available aptamer-based methods for analysis of OTC

Method	Materials	Analytical ranges	LODs	Instruments	Immobilization of aptamers (Y/N)	Ref
Electrochemical	Gold interdigitated array electrode chip	1–100 nM	1 nM	Electrochemical analyzer	Y	[13]
Electrochemical	Gold electrode	10–600 ng·mL^{-1}	9.8 ng·mL^{-1} (~20 nM)	Electrochemical analyzer	Y	[14]
Colorimetric	AuNPs	0.025–1 μM	25 nM	UV/vis spectrophotometer	N	[15, 16]
Light scattering	Polystyrene latex microspheres	10^2–10^4 ppb	100 ppb (~200 nM)	Microfluidic device and spectrometer	Y	[17]
Cantilever surface stress	Cantilever arrays	1–100 nM	0.2 nM	Cantilever sensor platform	Y	[18]
Fluorescence	Graphene	0.1–2 μM	10 nM	Spectrofluorimeter	N	This work

AuNPs Au nanoparticles, *Y* Yes, *N* No

repelled aptamer, which demonstrated that rGO was more appropriate as the quencher of labeled long-chain aptamer for establishing graphene-based fluorescent sensing platform.

Effect of potassium ion (K^+)

In this study, we reviewed the effect of K^+ on fluorescence restoration. As shown in Fig. 2, a distinct fluorescence intensity change was observed after the addition of K^+ in the phosphate buffer when detecting OTC. The reason was that this 76-mer size of OTC binding ssDNA aptamer was predicted to form one G-quadruplex structure which showed high affinity to OTC [11], and the G-quadruplex structure was stabilized by the presence of K^+ [35, 36]. This control experiment indicated that K^+ promoted the formation of G-quadruplex OTC complexes, which not only enhanced the space distance between rGO and dyes, but also increased the space charge density around the aptamer resulting in stronger G-quadruplex OTC complexes/rGO electrostatic repel interactions [37], thus inducing a higher fluorescence restoration.

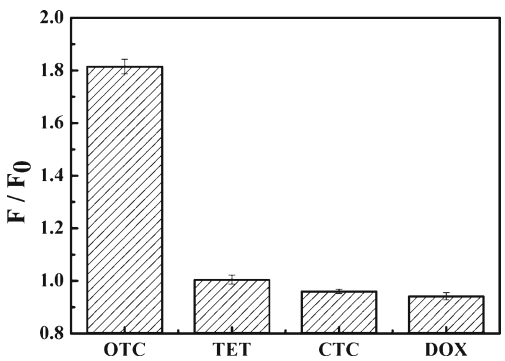

Fig. 5 Fluorescence intensity changes (F/F_0) in the presence of OTC (0.5 μM), TET (0.5 μM), CTC (0.5 μM) and DOX (0.5 μM), respectively. Where F_0 and F are the fluorescence intensity without and with OTC, TET, CTC and DOX respectively. Excitation: 494 nm, emission: 518 nm

Optimization of rGO concentration

From Fig. 3, with the increase in the concentration of rGO, the background fluorescence signal decreased gradually, indicating that the fluorescence quenching effect was directly related to the π-π stacking interaction between aptamer and rGO and the energy or electron transfer from dyes to rGO. Fluorescence quenching efficiency reached a plateau (92.2 %) after the rGO concentration exceeded 16 μg·mL^{-1}, indicating the FAM-labeled aptamer was completely absorbed onto the surface of rGO.

Therefore, 30 min reaction time, appropriate salt (Na^+, Mg^{2+}, K^+) in the phosphate buffer and 16 μg·mL^{-1} rGO were selected for the following analytical purposes.

Fluorescent detection of OTC

Under the optimal experimental conditions, the relationship between the OTC concentration and fluorescence enhancement was investigated. Figure 4a showed the fluorescence recovery in the presence of different concentrations of OTC. As indicated in Fig. 4b, the intensity of rGO-based assay increased with the increasing OTC concentration from 0.1 μM to 2 μM. The detection limit of 10 nM was estimated based on 3δ/slope criterion (δ, standard deviation of the blank samples). Table 1 summarized the analytical performance of aptamer-based methods for the detection of OTC. Since the

Table 2 Recoveries of OTC from lake water samples (n=3)

Sample	Standard value of OTC (μM)	Found (μM)	Recovery (%)	RSD (%, n=3)
Lake water	0.1	0.106	106	2.4
	0.2	0.195	97	0.6
	0.5	0.549	109	1.0

assay was carried out in homogeneous solution, it avoided the need for time-consuming immobilization, coating and washing steps in common heterogeneous assays, such as electrochemical [13, 14], light scattering [17] and microcantilever [18] methods. Furthermore, the sensitivity achieved in the present sensing system was higher than colorimetric [15, 16] method and some heterogeneous assays [14, 17]. Thus, this method would provide a rapid and sensitive approach for quantitative assay of OTC. Several reasons might explain the good analytical performance of this sensing platform. First, the ultrahigh fluorescence quenching ability of rGO led to a high signal-to-background ratio in comparison with aptamer-based colorimetric method, and thus high sensitivity for target detection could be achieved. Second, the formation of G-quadruplex OTC complexes enhanced the distance between FAM-labeled signal probe and the surface of rGO, inducing a higher fluorescence restoration upon the addition of target molecules at rather low concentrations. Third, the high affinity of the aptamer to its target molecules (in nanomolar range [16]) would be beneficial to detection of trace OTC. Furthermore, a relative standard deviation of 1.9 % (n=5, 0.1 μM OTC) was obtained, suggesting the good reproducibility of this method.

It was noteworthy that fluorescence intensity of FAM-labeled aptamer/rGO reached a plateau after the OTC concentration exceeded 2 μM. The adsorption of OTC onto the surface rGO via π-π interaction and cation-π bonding [38] might be the reason that responsible for not further improving the detection range.

Specificity of the method

To evaluate the specificity of this fluorescent assay, we investigated the effect of possible interferences which might interfere with the determination of target analyte OTC, including three structurally similar tetracycline derivatives (TET, CTC and DOX). In a typical experiment, the rGO-based assay was incubated with 0.5 μM OTC, 0.5 μM TET, 0.5 μM CTC and 0.5 μM DOX, respectively. As shown in Fig. 5, the relative fluorescence F_0/F for OTC was 1.81, while it was 1.01 for TET, 0.96 for CTC and 0.94 for DOX, where F_0 and F are the fluorescence intensity of the rGO FAM-aptamer solution without and with OTC, CTC and DOX, respectively. It was clear that the structurally similar tetracycline derivatives failed to cause a dramatic fluorescence change. The good selectivity of this method was attributed to the inherent specificity of aptamer toward OTC [16].

Detection of OTC in lake water samples

In order to evaluate the feasibility of its potential in the real aquatic environment, this fluorescent assay was applied to detect the OTC level in lake water (obtained from Xishan Lake, Dalian, China) samples. Prior to the sample analysis, lake water samples were pretreated using a 0.2 μm syringe filter to exclude the matrix effect caused by particulate or microbial cells. 200 μL of the lake water sample was mixed with 70 μL of the phosphate buffer containing FAM-labeled aptamer and incubated at room temperature for 30 min. Then 130 μL of 0.05 $mg \cdot mL^{-1}$ rGO was added to the above solution, which resulted in a solution with 16 $\mu g \cdot mL^{-1}$ rGO and 50 nM FAM-labeled aptamer. It was found the OTC content in the lake water was too low to be detected by this method. Hence extra OTC was added into the assay. The analytical results for the samples spiked with 0.1–0.5 μM of standard OTC were given in Table 2, the recovery was in the range of 97–109 %, which indicated that the developed method could be preliminarily applied for the determination of OTC in real samples (the results were calculated from the standard calibration curve in Figure S2 (ESM)).

Conclusions

In conclusion, a simple, selective and sensitive homogeneous fluorescent assay for OTC based on the OTC binding DNA aptamer and rGO is developed. We demonstrate for the first time that long-chain fluorescein-labeled DNA aptamer (76-mer) can be adapted to the sensitive and specific graphene-based fluorescent sensing platform by using water-dispersible rGO as an ultra highly efficient quencher. As to OTC, a sensitive detection limit of 10 nM is obtained with high specificity. On the basis of the excellent performance, this design can provide new insights for molecule recognition or contamination detection when long-chain aptamers is required as recognition units.

Acknowledgment This work was financially supported by the National Natural Science Foundation of China (No. 21277016).

References

1. Heilig S, Lee P, Breslow L (2002) Curtailing antibiotic use in agriculture. West J Med 176:9–11. doi:10.1136/ewjm.176.1.9
2. Gräslund S, Bengtsson BE (2001) Chemicals and biological products used in south-east Asian shrimp farming, and their potential impact on the environment — a review. Sci Total Environ 280:93–131. doi:10.1016/S0048-9697(01)00818-X
3. Himmelsbach M, Buchberger W (2005) Residue analysis of oxytetracycline in water and sediment samples by high-performance liquid chromatography and immunochemical techniques. Microchim Acta 151:67–72. doi:10.1007/s00604-005-0372-1
4. Aga DS, Goldfish R, Kulshrestha P (2003) Application of ELISA in determining the fate of tetracyclines in land-applied livestock wastes. Analyst 128:658–662. doi:10.1039/b301630g

5. Li YT, Qu LL, Li DW, Song QX, Fathi F, Long YT (2013) Rapid and sensitive in-situ detection of polar antibiotics in water using a disposable Ag-graphene sensor based on electrophoretic preconcentration and surface-enhanced Raman spectroscopy. Biosens Bioelectron 43:94–100. doi:10.1016/j.bios.2012.12.005
6. Kowalski P (2008) Capillary electrophoretic method for the simultaneous determination of tetracycline residues in fish samples. J Pharm Biomed Anal 47:487–493. doi:10.1016/j.jpba.2008.01.036
7. Vega D, Agüí L, González-Cortés A, Yáñez-Sedeño P, Pingarrón JM (2007) Voltammetry and amperometric detection of tetracyclines at multi-wall carbon nanotube modified electrodes. Anal Bioanal Chem 389:951–958. doi:10.1007/s00216-007-1505-7
8. Weber CC, Link N, Fux C, Zisch AH, Weber W, Fussenegger M (2005) Broad-spectrum protein biosensors for class-specific detection of antibiotics. Biotechnol Bioeng 89:9–17. doi:10.1002/bit.20224
9. Famulok M, Mayer G, Blind M (2000) Nucleic acid aptamers from selection in vitro to applications in vivo. Acc Chem Res 33:591–599. doi:10.1021/ar960167q
10. Iliuk AB, Hu L, Tao WA (2011) Aptamer in bioanalytical applications. Anal Chem 83:4440–4452. doi:10.1021/ac201057w
11. Sefah K, Phillips JA, Xiong X, Meng L, Van Simaeys D, Chen H, Martin J, Tan W (2009) Nucleic acid aptamers for biosensors and bio-analytical applications. Analyst 134:1765–1775. doi:10.1039/b905609m
12. Niazi JH, Lee SJ, Kim YS, Gu MB (2008) ssDNA aptamers that selectively bind oxytetracycline. Bioorg Med Chem 16:1254–1261. doi:10.1016/j.bmc.2007.10.073
13. Kim YS, Niazi JH, Gu MB (2009) Specific detection of oxytetracycline using DNA aptamer-immobilized interdigitated array electrode chip. Anal Chim Acta 634:250–254. doi:10.1016/j.aca.2008.12.025
14. Zheng D, Zhu X, Zhu X, Bo B, Yin Y, Li G (2013) An electrochemical biosensor for the direct detection of oxytetracycline in mouse blood serum and urine. Analyst 138(6):1886–1890. doi:10.1039/c3an36590e
15. Kim YS, Kim JH, Kim IA, Lee SJ, Jurng J, Gu MB (2010) A novel colorimetric aptasensor using gold nanoparticle for a highly sensitive and specific detection of oxytetracycline. Biosens Bioelectron 26:1644–1649. doi:10.1016/j.bios.2010.08.046
16. Kim YS, Kim JH, Kim IA, Lee SJ, Gu MB (2011) The affinity ratio—Its pivotal role in gold nanoparticle-based competitive colorimetric aptasensor. Biosens Bioelectron 26:4058–4063. doi:10.1016/j.bios.2011.03.030
17. Kim K, Gu MB, Kang DH, Park JW, Song IH, Jung HS, Suh KY (2010) High-sensitivity detection of oxytetracycline using light scattering agglutination assay with aptasensor. Electrophoresis 31(18):3115–3120. doi:10.1002/elps.201000217
18. Hou H, Bai X, Xing C, Gu N, Zhang B, Tang J (2013) Aptamer-based cantilever array sensors for oxytetracycline detection. Anal Chem 85(4):2010–2014. doi:10.1021/ac3037574
19. Geim AK, Novoselov KS (2007) The rise of graphene. Nat Mater 6:183–191. doi:10.1038/nmat1849
20. Gan T, Hu S (2011) Electrochemical sensors based on graphene materials. Microchim Acta 175(1–2):1–19. doi:10.1007/s00604-011-0639-7
21. Swathi RS, Sebastian KL (2008) Resonance energy transfer from a dye molecule to graphene. J Chem Phys 129:054703–054709. doi:10.1063/1.2956498
22. Swathi RS, Sebastian KL (2009) Long range resonance energy transfer from a dye molecule to graphene has (distance)$^{-4}$ dependence. J Chem Phys 130:086101–086103. doi:10.1063/1.3077292
23. Lu CH, Yang HH, Zhu CL, Chen X, Chen GN (2009) A Graphene platform for sensing biomolecules. Angew Chem Int Ed 48:4785–4787. doi:10.1002/anie.200901479
24. Perez-Lopez B, Merkoci A (2012) Carbon nanotubes and graphene in analytical sciences. Microchim Acta 179:1–16. doi:10.1007/s00604-012-0871-9
25. Morales-Narváez E, Merkoçi A (2012) Graphene oxide as an optical biosensing platform. Adv Mater 24:3298–3308. doi:10.1002/adma.201200373
26. Chang H, Tang L, Wang Y, Jiang J, Li J (2010) Graphene fluorescence resonance energy transfer aptasensor for the thrombin detection. Anal Chem 82:2341–2346. doi:10.1021/ac9025384
27. He Y, Lin Y, Tang H, Pang D (2012) A graphene oxide-based fluorescent aptasensor for the turn-on detection of epithelial tumor marker mucin 1. Nanoscale 4:2054–2059. doi:10.1039/c2nr12061e
28. Liu C, Wang Z, Jia H, Li Z (2011) Efficient fluorescence resonance energy transfer between upconversion nanophosphors and graphene oxide: a highly sensitive biosensing platform. Chem Commun 47:4661–4663. doi:10.1039/c1cc10597c
29. Wu M, Kempaiah R, Huang PJ, Maheshwari V, Liu J (2011) Adsorption and desorption of DNA on graphene oxide studied by fluorescently labeled oligonucleotides. Langmuir 27:2731–2738. doi:10.1021/la1037926
30. He S, Song B, Li D, Zhu C, Qi W, Wen Y, Wang L, Song S, Fang H, Fan C (2010) A Graphene nanoprobe for rapid, sensitive, and multicolor fluorescent DNA analysis. Adv Funct Mater 20:453–459. doi:10.1002/adfm.200901639
31. Mehta J, Rouah-Martin E, Van Dorst B, Maes B, Herrebout W, Scippo ML, Dardenne F, Blust R, Robbens J (2012) Selection and characterization of PCB-binding DNA aptamers. Anal Chem 84:1669–1676. doi:10.1021/ac202960b
32. Jo M, Ahn JY, Lee J, Lee S, Hong SW, Yoo JW, Kang J, Dua P, Lee DK, Hong S, Kim S (2011) Development of single-stranded DNA aptamers for specific Bisphenol A detection. Oligonucleotides 21:85–91. doi:10.1089/oli.2010.0267
33. Sun X, Liu Z, Welsher K, Robinson J, Goodwin A, Zaric S, Dai H (2008) Nano-graphene oxide for cellular imaging and drug delivery. Nano Res 1:203–212. doi:10.1007/s12274-008-8021-8
34. Zhou Y, Bao Q, Tang LAL, Zhong Y, Loh KP (2009) Hydrothermal dehydration for the "green" reduction of exfoliated graphene oxide to graphene and demonstration of tunable optical limiting properties. Chem Mater 21:2950–2956. doi:10.1021/cm9006603
35. Sen D, Gilbert W (1990) A sodium-potassium switch in the formation of four-stranded G4-DNA. Nature 344:410–414. doi:10.1038/344410a0
36. Walmsley JA, Burnett JF (1999) A new model for the K^+-induced macromolecular structure of guanosine 5′-monophosphate in solution. Biochemistry 38:14063–14068. doi:10.1021/bi9900370
37. He F, Tang Y, Wang S, Li Y, Zhu D (2005) Fluorescent amplifying recognition for DNA G-quadruplex folding with a cationic conjugated polymer: a platform for homogeneous potassium detection. J Am Chem Soc 127:12343–12346. doi:10.1021/ja051507i
38. Gao Y, Li Y, Zhang L, Huang H, Hu JJ, Shah SM, Su XG (2012) Adsorption and removal of tetracycline antibiotics from aqueous solution by graphene oxide. J Colloid Interface Sci 368:540–546. doi:10.1016/j.jcis.2011.11.015